Perspectives on manufacturing simulations of Li-S battery cathodes

Journal of Physics: Energy

OPEN ACCESS

RECEIVED
3 November 2021

REVISED
16 December 2021

ACCEPTED FOR PUBLICATION
12 January 2022

PUBLISHED
15 March 2022

PERSPECTIVE

Perspectives on manufacturing simulations of Li-S battery cathodes

Oier Arcelus[1,2,3,4] **and Alejandro A Franco**[1,2,5,6,*]

[1] Laboratoire de Réactivité et Chimie des Solides (LRCS), CNRS UMR 7314, Université de Picardie Jules Verne, Hub de l'Energie, 15 rue Baudelocque, 80039 Amiens Cedex, France
[2] Réseau sur le Stockage Electrochimique de l'Energie (RS2E), Fédération de Recherche CNRS 3459, Hub de l'Energie, 15 rue Baudelocque, 80039 Amiens Cedex, France
[3] Centre for Cooperative Research on Alternative Energies (CIC energiGUNE), Basque Research and Technology Alliance (BRTA), 01510 Vitoria-Gasteiz, Spain
[4] Institut de Ciència de Materials de Barcelona,` ICMAB-CSIC, 08193 Bellaterra, Spain
[5] ALISTORE-European Research Institute, Fédération de Recherche CNRS 3104, Hub de l'Energie, 15 rue Baudelocque, 80039 Amiens Cedex, France
[6] Institut Universitaire de France, 103 Boulevard Saint Michel, 75005 Paris, France
[*] Author to whom any correspondence should be addressed.

E-mail: alejandro.franco@u-picardie.fr

Keywords: lithium sulfur batteries, manufacturing, computational modeling, electrode mesostructure

Abstract

Lithium-sulfur batteries (LSBs) are one of the main contenders for next generation post lithium-ion batteries (LIBs). As the process of scientific discovery advances, many of the challenges that prevent the commercial deployment of LSBs, especially at the most fundamental materials level, are slowly being addressed. However, batteries are complex systems that require not only the identifcation of suitable materials, but also require the knowledge of how to assemble and manufacture all the components together in order to obtain an optimally working battery. This is not a simple task, as battery manufacturing is a multi-stepped, multi-parameter, highly correlated process, where many parameters compete, and deep knowledge of the systems is required in order to achieve the optimal manufacturing conditions, which has already been shown in the case of LIBs. In these regards, manufacturing simulations have proven to be invaluable in order to advance in the knowledge of this exciting and technologically relevant field. Thus, in this work, we aim at providing future perspectives and opportunities that we think are interesting in order to create digital twins for the LSB manufacturing process. We also provide comprehensive and realistic ways in which already existing models could be adapted to LSBs in the short-term, and which are the challenges that might be found along the way.

1. Introduction

Commercially extended energy storage technologies such as the lithium-ion battery (LIB) has supposed a revolution in terms of the surge of portable electronics and clean mobility applications such as the electric vehicle [1–3]. First commercialized by Sony in 1991, LIBs have come a long way and have pushed their limits close to the theoretical ones [4] delivering energy densities in the range of ∼250 Wh kg^{-1}. This is a titanic achievement; however, it is barely sufficient to meet the society's demands on long-ranged transportation and green energy.

In these regards, lithium-sulfur batteries (LSBs) appear to be a promising candidate for post LIBs [5–7], due to the abundance of sulfur resources, their low cost, and their nontoxicity. In fact, LSBs show theoretical energy densities (2600 Wh kg^{-1}), far superior to their LIB counterparts. However, their widespread deployment has been hindered by several technical issues.

At the materials level, the main challenges that need to be tackled are the following: (a) the insulating nature of elemental sulfur (S_8) and the precipitated discharge product lithium sulfide (Li_2S) [8], which

requires the use of large amounts of carbon additives; (b) the ubiquitous polysulphide (PS) shuttle effect, where highly soluble intermediate PSs diffuse to the anode to form Li_2S, and thus result in a loss of capacity, poor cyclability, and fast self-discharge [9–12]. Here, strategies to block the PS from diffusing to the anode involve, among others, the engineering of the conductive carbon–sulfur (C/S) composite complexes that restrain PS diffusion to their internal porosity [13–16], finding electrolytes with low PS solubility [17, 18], and fabricating separators that act as barriers against the PS diffusion [19, 20]; (c) the incorporation of Li metal as anode material, which induces dendrite formation, and poses additional challenges in the formation of protective solid electrolyte interfaces (SEIs) [21, 22].

At the cathode manufacturing level, given their equivalent processing steps for LIBs and LSBs [23], it is tempting to believe that the optimization of LSB cathodes may follow the same steps as those of the LIB cathodes. However, due to the drastic differences between the working principles of the solvent mediated reactions of LSBs and the intercalation reactions in LIBs, the requirements for efficient C/S composite cathodes are also quite different. For instance, we center our attention to the porosity of the C/S composite cathodes, which is considered as a key parameter to optimize the energy density of LSBs [24]. Cathode porosity is controlled by calendering the as-dried electrode after the previous casting of the slurry onto the current collector (CC). It affects the sulfur utilization, by varying the electrolyte to capacity (E/C) ratio, and the accessible carbon surface area, which influences the overall achievable capacity. It also has profound effects on the discharge polarization and cycle life. Furthermore, the electrode porosity is a key parameter that controls the electrolyte to sulfur (E/S) ratio, which is also one of the main factors to consider when trying to optimize the energy density of LSBs at the cell level [25]. Indeed, as stated by Bhargav *et al* a 50% increase in the specific energy density of the cell can be achieved by lowering the E/S ratio from 5 to 2 μl mg^{-1}, for a given sulfur loading [25].

Modeling has made important contributions when it comes to understanding the operational principles of LSBs from both, the materials, and mechanistic perspectives. Atomistic and molecular dynamics simulations have focused on understanding the interactions between salts, solvents and PS species [26, 27], and on elucidating their interactions with carbon or other conductive supports [28]. Moreover, continuum models of LSBs have been valuable in shedding light on the PS reaction steps and limiting factors of battery cell operation [11, 29–32]. However, models that simulate the operation of LSBs in relation to the cathode mesostructure are more scarce. Some continuum models account for the C/S electrode's inter- and intra-particle meso- and micro-porosity, and analyze the cell performance with respect to variations in the textural properties of the electrodes [33, 34]. These models qualitatively capture general experimentally observed trends of LSB operation, and shed light on the physical reasons that limit the capacity of such batteries (pore clogging, decrease of active surface area, etc.). Still, they consist of 1D homogenized models that do not account for the 3D nature of the heterogeneities of the C/S composite electrodes or the Li_2S deposits. In these regards, Mistry *et al* developed a model where stochastically generated 3D C/S electrode mesostructures functioned as hosts for the Li_2S discharge precipitates [35]. Concretely, they used a control parameter that defined the 'film'- or 'finger'-like 3D morphology of the stochastically generated Li_2S deposits. Of course, these deposits induced changes in the electrode mesostructure, which were implicitly considered in a coupled 0D electrochemical model. Additionally, Vigneshwaran *et al* from our group developed a kinetic Monte Carlo (kMC) model where dissolution, precipitation, diffusion and electrochemical reaction events were resolved in a stochastically generated 3D carbon-based electrode mesostructure [36]. This model fully couples Li_2S deposit formation, mesostructural changes, and electrochemical performance in 3D, and is able to analyze various cell operation and initial conditions, such as applied C-rates and S loadings. Lastly, reactive molecular dynamics (ReaxFF) models have also been developed, where the trajectories of sulfur and carbon based supports are simulated [37]. The model captures the reactions of sulfur, volume expansion, and discharge potentials in a small region of the microporosity of the carbon. Thus, it is a more local approach when compared to the above-mentioned works.

All the works cited above show that the ongoing efforts to model the operation of LSBs, and particularly those that link mesostructure/performance relationships, have resulted in novel insights and potential design principles for batteries with improved performance. However, a missing common link of all these models is the way in which the 3D electrode mesostructures are obtained in the first place. As shown, most of the works rely on the stochastic generation of mesostructures with some selected mesostructural properties (e.g. porosity). Instead, electrode mesostructures are a direct result of their manufacturing. Again, manufacturing steps such as calendering (figure 1(A)) are directly correlated to the C/S electrode porosity, which is vital to optimize the specific energy density of LSBs [24]. Therefore, the mesoscale modeling paradigm, shown in figure 1(B), takes full form also in the field of LSBs [38]. Indeed, modeling the relationships between mesostructural properties and manufacturing conditions is a practically unexplored field for LSBs, and this work aims at providing future perspectives, challenges, and opportunities on this issue.

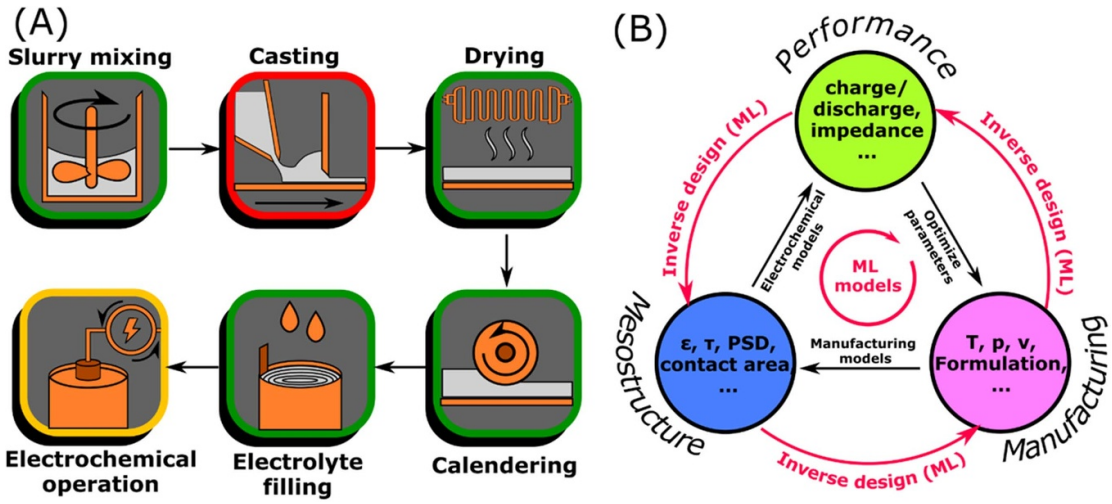

Figure 1. (A) LSB (and LIB) manufacturing steps that are prone to highly affect the mesostructural properties of the resulting electrodes, and thus the steps which are interesting to analyze from a mesoscale simulation perspective. The green squares represent the manufacturing steps for which experimentally validated LIB digital twins exist and are directly applicable to LSBs, with a few tweaks. The red squares represent the manufacturing steps for which no digital twins exist outputting an explicit mesostructure, for example by using CGMD simulations. Yellow squares represent the steps for which LIB models exist but require from brand new approaches to be able to simulate LSBs in 3D. (B) Our interpretation of the mesoscale modeling paradigm. The pink, blue, and green nodes represent the manufacturing conditions, mesostructural properties, and electrochemical performance of LSBs. Straight black arrows represents the ways in which each node feeds the other. Clockwise pink arrows represent the way machine learning (ML) models can be used to accelerate the physical models. Counter-clockwise pink arrows represent the way ML models could be used for inverse design.

2. Manufacturing models

LSBs pose very interesting and challenging problems for the modeling of the manufacturing process. Battery manufacturing generally depends on the type of battery technology. As pointed out by Duffner *et al* many of these technologies have, for the most part, compatible manufacturing processes when compared to mature LIB technologies [23]. Overall, LSBs are one of those technologies (figure 1(A)) even if, as stated earlier, the requirements of the C/S composite electrodes for LSBs may be different. In these regards, the LIB manufacturing modeling field has bloomed in the past few years, in particular in the context of the ERC-funded project ARTISTIC [39], that aims at providing digital twins to the manufacturing processes of LIBs. In the digital twins developed at the ARTISTIC project, the manufacturing related simulations are implemented in a data pipeline that takes manufacturing conditions of LIB electrodes as an input (formulation, drying rates, calendering pressures…), and generates realistic, experimentally validated, simulated electrode mesostructures as an output. In the following, we discuss how each of the steps of this existing computational workflow could be adapted to the LSB cathode manufacturing, along with the challenges and perspectives to perform these simulations.

2.1. Slurry simulations

The preparation of homogeneous slurries with good rheological properties is crucial to obtain well behaved electrodes without cracks or undesired delamination from the CC. The formulation of the slurry is, in fact, a limiting factor in terms of production times of LIBs [40]. From the modeling point of view, several of our works have simulated slurries containing nickel–manganese–cobalt (NMC) as active material (AM) for LIB cathodes by means of coarse-grained molecular dynamics (CGMD) [41–43]. These simulations represent the various components that form the slurry as particle beads. For instance, one of these approaches considers the AM secondary particles as single particle beads, while the conductive carbon additives, binder, and solvent, are represented in the so-called carbon-binder domain (CBD) particle beads. Another possible approach is to build a slurry model that includes the carbon particles explicitly [44]. Then, the CBD particles are separated into solvent + binder and carbon aggregate beads, which allows following the process of carbon additive agglomeration in the slurry. The CGMD method defines the means by which all the above-listed components of the slurry physically interact with each other via force fields (FFs). The FFs may be defined in a variety of ways. For instance, many of the abovementioned works use a combination of Lennard-Jones (LJ) and granular Hertzian (GH) FFs. We note that the choice of the FFs depends on the application. However, any CGMD model, that attempts to simulate realistic slurries, needs to select the parameters of the FFs such

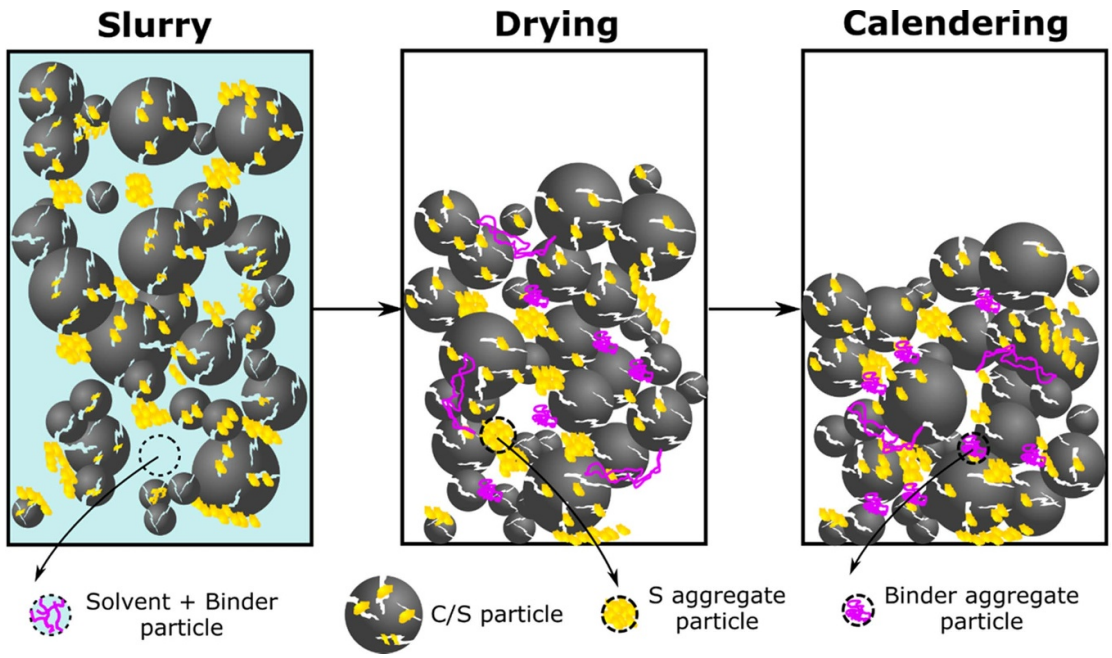

Figure 2. (Top) Schematic representation of the mesostructures obtained through slurry, drying, and calendering simulations. (Bottom) A plausible way of coarse graining the different constituent phases of an LSB electrode for CGMD simulations.

that the simulated slurries reproduce their real experimental properties. From the experimental point of view, the slurry rheology is an important aspect that affects the manufacturing process, as it affects the coating process and the final electrode mesostructures [45]. In these regards, non-equilibrium molecular dynamics simulations have been used to parameterize the FFs and fit the rheological properties of the slurries, such as the viscosity vs shear-rate curves, as a validator for the slurry models. This experimental validation is one of the largest bottlenecks in the development of manufacturing digital twins, as it requires exploring the FF parameter space to find the best fit for the viscosity versus applied shear-rate curves. In these regards, optimization algorithms, such as the particle swarm optimization and ML models have been applied to accelerate this fitting process (figure 1(B)) by a factor of 20 [42].

In the context of LSBs, as we already mentioned, nanostructured C/S composite cathodes are vital in order to improve sulfur utilization [13]. However, when using nanosized materials, it is difficult to form well dispersed slurries and uniform coatings without cracks or pinholes [8], which limits the achievable sulfur loadings ($\sim$2 mg cm^{-2}) of the electrodes and thus hinders their application range. From the slurry modeling perspective, nanosized particle beads also pose problems as the number of particles to simulate quickly becomes intractable for relatively small simulation domains [44]. This makes it computationally prohibitive to obtain mesostructural models with characteristic sizes larger than $\sim$1 μm. Fortunately, some modern strategies to obtain well behaved, easy to cast electrodes, with higher sulfur loadings, rely on synthesizing secondary structures with μm-sized features [8, 46–48]. Therefore, we think that the process by which slurry models are obtained in the context of LIBs, which we mentioned above, are directly applicable to LSB slurries, where AM particles would be composed of μm-sized C/S composite beads, and eventually free elemental sulfur aggregates, that will later occupy the mesoporosity of the electrodes instead of the carbon microporosity. The latter will have to be accounted for through effective properties of the C/S composite beads, as shown in figure 2. One additional point that should be considered is that LSBs electrodes can include a large variety of nanostructured materials with shapes that largely differ from spheres, i.e. nanofibers, nanotubes, nanosheets, etc. In all these cases, the size-limiting considerations that we made still stand. This means that particle beads with nanosized features, regardless of their shape, pose problems for simulating small to moderate volume simulation domains, due to the associated computational costs. However, we note that the simulation of LSB (or LIB) slurries is not only limited to spherical particles. Indeed, simulating arbitrarily shaped particle beads is possible with the multi-sphere approach, as long as the particle features are μm-sized. In this case the main particles would be formed using aggregates of smaller overlapping spherical particles [49]. Such approach would allow to reproduce particle shapes such as fibers, platelets, tubes, etc.

2.2. Drying simulations

After the slurry is formed, the coated electrode is dried in order to remove all the solvent and form an uncalendered electrode (figure 2). Again, drying is one of the most expensive processes to manufacture LIBs, both in terms of overall economic and energetic costs [40]. Therefore, applying high drying rates is of industrial interest as it has the potential to save manufacturing times and costs. However, it is proven that drying rates largely affect the properties of the resulting electrodes [50–53]. Concretely, it is shown that high drying rates promote the formation of gradients of binder and carbon phases by convective and capillary forces, where both carbon and binder additives migrate towards the top of the electrode by depleting the CC side. These gradients result in more brittle electrodes with low adhesion to the CC. Additionally, from the mesostructural perspective, the inhomogeneous distribution of carbon and binder additives leads to altered electronic and ionic percolation paths, which ultimately affect the electrochemical performance of the electrodes [54]. Understanding additive migration is therefore of paramount importance to come up with strategies and protocols to improve the performance and lower the fabrication costs of LIBs. In these regards, modeling could become a useful tool to study complex phenomena related to electrode drying [54–57].

In the context of the ARTISTIC project, we recently developed the first ever 3D physics-based model that accounts for carbon-binder migration as a function of the applied drying rates on LIB electrode mesostructures [58]. The model is implemented as the second stage in the manufacturing workflow, where the experimentally validated slurry mesostructure that we described in section 2.1 is used as an input for the drying model. Similar to the slurry model, the drying process is simulated using CGMD. In this case, the dynamics of the system take place while the CBD particles shrink at a certain rate, which is defined as the ratio between time needed to remove all the solvent from the CBD particles and the total simulation time. Concretely, the most important factors that are considered when setting up the drying model are the following: (a) The solvent evaporation is asymmetric along the thickness of the electrode, (b) the physical properties of CBD particles change as the solvent is removed, and (c) particle sedimentation is considered across the whole simulation time. Point (a) is built on the realization that solvent evaporation is faster in the top of the electrode than in the bottom part. Therefore, three regions are initially set in the slurry, each encompassing one third of the electrode thickness. Then, three different shrinking rates are defined for the CBD particles in each of the regions, where the CBD particles on the upper-most region shrink faster than the ones in the bottom part. Point (b) is implemented by increasing the density of the CBD particles as the solvent is removed from them. Most importantly, the attractive interactions between the CBD particles are also increased upon drying, thus mimicking convection and capillary forces because of the application of asymmetric drying rates. Lastly, in point (c), the particle sedimentation is considered by including an additional effective downwards force on each of the particles in the simulation domain, which forces the particles to sediment on the bottom of the simulation box. The resulting dried electrodes reproduce the additive migration phenomena, which changes as a function of the applied drying rates. It can also be used to analyze the effect of more complex drying protocols onto the mesostructural properties and electrochemical performance of the resulting electrodes.

Drying protocols and their effects on the mechanical and electrochemical properties of the LSB electrodes are much less studied, due to the lack of wide industrial maturity of the LSB technology. However, given the equivalent processing steps for LSB and LIB electrodes [23], it is highly likely that some of the same computational simulation concepts that are developed for LIBs are applicable to LSBs. One of the main distinguishing factors that we think could affect the way drying protocols are set up, lies in the fact that C/S composite electrodes usually carry higher additive amounts when compared to LIB electrodes, where many of the works in the literature report binder additive contents of ∼20 w.t % [8, 24, 25, 46, 47, 59]. We note that a common conclusion from the drying experiments and simulations for LIBs, is that the formation of the carbon and binder additive gradients does not happen all along the drying process. Instead, additives migrate at very specific times during drying [50, 58, 60]. Drying protocols are developed by changing the drying rates as a function of the expected additive mobility, being the drying rate high when no additive migration is expected, and vice versa. However, these timeframes for additive migration, and their respective onsets, will change, not only as a function of the properties of the additives and their interactions with respect to the rest of electrode components, but also as a function of the sheer quantity of them. Indeed, it is shown that increasing binder amounts in graphite slurries result in higher internal stresses upon drying [61]. In this scenario, it is unclear whether additive migration will be facilitated or hampered by increasing additive amounts. It is also unclear whether the timeframes for migration will be shrunk or expanded, or the onsets will be advanced or delayed. This would ultimately define which drying protocols to use in each case. Additionally, depending on the solvent and binder chemistries that are used, the cohesive and granular interactions between the constituent phases of the electrode will also change, mimicking the changes in the convective and capillary forces that happen inside the electrodes. This might affect the abovementioned

simulated migration onsets and timeframes. We speculate that highly cohesive additives will likely result in delayed migration onsets and lower additive gradients, while the contrary might happen with the less cohesive ones. Another potential consideration lies in the fact that, depending on the solvent used, drying temperatures can be rather high. Aqueous slurries are not the case given its low boiling point. However, other industrially relevant solvents, such as N-methylpyrrolidone (NMP), have boiling points around 200 °C, which is well above the boiling point of elemental sulfur (155 °C). This could result in some degree of sulfur loss, due to the molten sulfur being in equilibrium with its vapor and thus escaping the electrode in gas form. Additionally, it has been shown by thermogravimetric analysis, that the temperature onset for sulfur volatilization in a variety of carbon/sulfur composites lies around 200 °C [48, 62], which could potentially result in a loss of AM during drying. These effects should be considered in the simulations by accounting for the total mass loss of each AM particle bead. Lastly, accounting for the effect of particle size and shape on the behavior of the electrode upon drying is also another problem worth exploring. A common conclusion of some of the experiments that show the drying process on LIB electrodes is that, after the initial shrinking of the electrode due to solvent evaporation, the formation of liquid capillaries inside the pore network dominates the subsequent stages of the drying process, where the additive migration happens [52, 53]. At this stage, forming well connected capillaries seems necessary for a complete and effective drying. Otherwise, isolated liquid-filled pores remain inside the pore structure, and the drying will now depend on the evaporation and gas-diffusion of these small solvent clusters through the electrode's pore network, which reduces the overall drying rate of the electrodes. This strong dependence of the electrode's pore network on the drying process clearly suggests that the size and shape of the AM particles will largely affect the drying process [52]. Moreover, Liu *et al* used kMC simulations to show that visible differences arise between the evaporation rates of LIB electrode microstructures containing particles of spherical, polyhedral, and cubic shapes [55]. Therefore, in a similar fashion, we would also expect to see these differences in the drying behavior of LSB battery electrodes composed of C/S composite particles beads of arbitrary shapes by using the multi-sphere approach. We would also expect to see differences between the different orientations that they may have with respect to the CC, i.e. isotropic, parallel, perpendicular, etc. With all the above considerations, we think that, as in the case of slurry simulations, the presented drying model is directly applicable to the case of LSBs and can help researchers explore the potential scenarios we introduced in this section.

2.3. Calendering simulations

Electrode calendering is another fundamental step in the battery manufacturing process, where the as-dried coated electrode is compressed in order to obtain the desired electrode properties. In LIBs, electrode calendering results in electrodes with lower porosities and better interparticle contacts (figure 2), which improves the electronic percolation networks within the mesostructures. This step is necessary to optimize the volumetric energy and power densities of the cells [63–68]. However, too extreme compressions are also found to be detrimental, since low porosity electrodes lead to higher tortuosity factors that hinder ionic diffusion within the electrolyte phase, thus resulting in reduced power densities. Therefore, it is important to find the optimal porosity, which represents a trade-off between the above-mentioned factors. Of course, the way in which porosity, and other mesostructural properties, are affected by calendering, depends on the electrode properties themselves, such as the composition, the physical interactions between the constituent particles, the overall Young modulus and hardness, etc.; and the calendering conditions, such as the pressure, temperature of the rolls, and line speed [64]. Finding these relations experimentally is a cumbersome process, which requires from systematic experiments that sample complex parameter spaces for different formulations, materials, and manufacturing conditions. This brute force trial and error approach is very costly in terms of development times, and resources. Thus, realistic physical models of the calendering process can serve as effective tools to inform on suitable experimental conditions for optimally calendered electrodes at a fraction of the original cost.

The physical models for the calendering process are generally built using the discrete element method (DEM) [69–73]. However, most of them rely on an implicit description of the CBD phase within the electrode, or on stochastically generated electrode mesostructures. On the contrary, our approach allows obtaining experimentally validated slurries and their corresponding dried electrodes as explained earlier, which explicitly track the position of the AM and CBD particles along the manufacturing process. This is found to be critically important for electrodes where the AM particles have intrinsically low electronic conductivities, such as transition metal oxides, where the explicit CBD network is highly correlated with the electronic conductivity of the electrode [74]. Thus, we implement a step further in the digital twin of the electrode manufacturing process by building a calendering model for the dried electrodes [43]. The dried electrodes are then embedded into a DEM model where two granular walls are included at the top and the bottom of the simulation box to model the calendering roll and the CC. The DEM model substitutes the

cohesive LJ FFs, that we used previously in the slurry and drying CGMD models, by a granular simplified Johnson-Kendall-Roberts (SJKR) [75] FF, which simulates a system where interparticle interactions depend directly on their contacts. An intrinsic advantage of using a combination of GH and SJKR FFs is that their parameters are now directly related to the macroscopic mechanical properties of the constituent materials that are simulated, such as their Young modulus (E) and Poisson ratio (ν), among others. Lastly, the parameterization of the FFs and model validation is done by fitting two different experimental observables: (a) micro-indentation curves, where the load that is felt by a micro-indenter is plotted versus the penetration displacement into the testing material. This is achieved computationally by moving the top-most plane into the electrode and recording the force that is exerted by the particles onto the moving wall due to such compression; and (b), electrode porosity evolution as a function of the calendering pressure (compaction curves), where the top-most plane is moved back into its initial position after compressing the electrode, allowing the electrode to relax. In this case, the calendering simulation captures both the plastic deformation and elastic recovery of the compressed electrode. This experimental validation ensures that the mechanical properties of the model electrode are consistent with the experiments, and that their mesostructural properties, such as the porosity, are consistently linked with fabrication conditions such as calendering pressures.

We already insisted on the fact that electrode porosity is a key property when designing optimal LSB electrodes. High electrode porosities for the same sulfur loading increase the E/S ratio, and thus improve sulfur utilization at the cost of the added weight, which is found to be detrimental for the cell energy density [24, 25]. In contrast, porosities that are too low reduce the amount of electrolyte available for sulfur dissolution, and thus the electrolyte reaches its saturation point faster, reducing sulfur utilization and increasing the E/C ratio. Additionally, the available active surface area is also lowered, resulting in electrodes that rapidly get electronically passivated due to the insulating nature of the Li_2S deposits. Therefore, our calendering model offers a valuable tool that allows to analyze how electrode porosity evolves as a function of the applied calendering pressures for LSB cathodes. However, in the following we list some of the challenges that may appear when trying to adapt the existing model to LSB cathodes. The main difference that we might encounter is that C/S composites have mechanical properties that are vastly different to Li-based transition metal oxides that are used as AMs in LIB cathodes. For instance, the Young modulus of NMC ranges between 100 and 200 GPa [70, 76, 77] In contrast, while we could not find clear studies on the mechanical properties of C/S composites in terms of their Young moduli specifically for LSBs, porous carbon materials are found to have Young moduli on the range of $\sim$10 GPa, which generally have a direct negative correlation with their internal porosity [78–80]. Meaning that mesoporous carbons of high porosities will tend to be softer. Additionally, the Young modulus of amorphous Li_xS alloys is calculated to increase from 15 to 45 GPa when increasing Li content [81]. Thus, we are inclined to believe that, depending on the calendering pressures, the spherical approximation for the C/S composite particle beads might no longer be appropriate, since they would be prone to suffering large deformations (and even cracking and disaggregation for the sulfur) when subject to compressive loads. Formally, this is even the case for NMC cathodes [70], but the effect could become even more pronounced with the potentially lower Young moduli of the C/S composite particles. A possible way of adapting the DEM models for C/S composites could be to consider a multi-sphere method as previously introduced in section 2.1 [49]. This method not only will allow to better reproduce the realistic shape of the particles, but, with a few tweaks, such as including bonds between the smaller overlapping particles, or increasing the cohesive interactions between them, one might be able to also reproduce the changes on the shapes of the main particles upon compressive stresses, which could solve the problem of considering rigid spherical AM particles.

2.4. Electrolyte infiltration simulations

In the LIB manufacturing chain, calendered electrodes are further processed and assembled into cells, where a variety of intermediate steps are taken, such as slitting, vacuum drying, cutting, etc [23]. The final steps of the battery manufacturing process involve electrolyte wetting and formation, which are two of the most time consuming and economically costly manufacturing steps [40, 82]. Concretely, electrolyte wetting is critically important for the following reasons: (a) the electrolyte must cover as much of the AM surface as possible, in order to allow for (dis)charge transfer reactions to occur, meaning that the electrochemically active surface area is determined by how well the electrolyte wets the electrode, thus affecting electrochemical performance both in terms of energy densities and rate capabilities [83]; (b) having well wetted electrodes is vital for the controlled and homogeneous formation of protective AM/electrolyte interfacial layers, such as the SEI and the cathode electrolyte interface, whose incomplete or inhomogeneous formation can result in a reduced battery cycle life [84]. Therefore, trying to understand which parameters affect the process of electrolyte filling becomes exciting and relevant to study, where some experimental works are already shedding light into this issue [85–92].

Obtaining well wetted electrodes is also important for the practical applicability of LSBs. As already stated, the sulfur conversion reaction happens through dissolution of elemental sulfur into long and intermediate chain PSs (Li_2S_x where $x \geqslant 4$), and their subsequent reduction and precipitation of insoluble Li_2S. This solution mediated reaction requires the elemental sulfur to be in direct contact and fully surrounded by the electrolyte [25]. Additionally, we also mentioned that the E/S ratio is a key parameter to optimize the energy density of LSBs. However, the E/S ratio alone cannot predict the degree of sulfur utilization. Assuming fully wetting conditions, low E/S ratios are expected to increase the E/C ratios, due to reaching saturation for the dissolved PSs faster, and thus limiting the achievable capacity. This trade-off is exacerbated when considering the additional hydrophobicity of the conductive carbon supports of LSB cathodes, which further increases the E/C ratios due to the presence of electrochemically inactive unwetted regions in the electrode. Moreover, the dissolution of the PSs themselves are found to change the properties of the electrolytes, by increasing their viscosities and thus further reducing their wettability [93].

Therefore, studies that specifically focus on the electrolyte impregnation process and that try to find strategies to improve the wettability of the electrodes are desirable in order to better their performance [93, 94]. However, to the best of our knowledge for LSBs, there is no imaging studies in the literature that directly follow the path of the electrolyte in real time, neither at the cell nor at the mesoscale level. Therefore, focusing on understanding the way that the electrolyte penetrates, and wets the internal electrode pores and surfaces, becomes relevant to design new cathode architectures and electrolyte formulations that improve the wettability of the LSB cathodes, thus improving sulfur utilization and lowering the E/C ratios.

In these regards, simulating the electrolyte infiltration process can be useful to obtain a deeper understanding on the role that the electrode's textural properties, and the electrolyte's properties have on the wetting behavior of the electrodes. In the ARTISTIC project, this is achieved for LIB electrode mesostructures, by using the lattice Boltzmann model (LBM) [95] to simulate porous media flow. The LBM is a fluid dynamics simulation tool that accounts for both, the macroscopic fluid flow, via the Navier–Stokes equation, and the microscopic interactions of the fluid particles with themselves and the rest of the surrounding fluid and solid phases, through various parameters, such as fluid densities, fluid viscosities, liquid contact angles, applied external forces etc [96]. It is therefore suitable for multi-phase flow simulations, where the infiltrating electrolyte has to interact with all the different phases that constitute an LIB electrode and the air initially present in the pores [97]. The first attempts that applied the LBM to LIB electrode mesostructures were done in 2D [98, 99]. These studies showed that the mesostructural properties of the electrode themselves were critical for the wettability of porous electrodes. Changes in the porosity, tortuosity, and pore size distributions, which are controlled by particle shapes and sizes, electrode formulation, and previous manufacturing conditions, could be used to tune the properties of porous electrodes. Indeed, Mohammadian *et al* showed by LBM simulation that including straight microchannels in the electrodes improved wettability and boosted the thermal performance of LIBs [100]. This is also shown to improve the volumetric energy density of LIBs [101]. Heterogeneities at the mesoscale are also shown to be important for the wettability of porous electrodes. For instance, Mukherjee *et al* used two phase LBM simulations to simulate water intrusion in carbon paper gas diffusion layer (GDL) and catalyst layer (CL) mesostructural models with applications for polymer membrane fuel cells. They showed the formation of highly heterogeneous water fronts that followed the less tortuous pathways along a preferred orientation within the GDL mesostructures. They also showed the existence of a capillary fingering, and a flat, front-like, water intrusion regimes on the CL mesostructures, that depended on the exerted capillary pressure. In a similar fashion, our works further extended these models to 3D simulations for LIB electrodes, where the CBD spatial location was explicitly considered [102]. In our work, the sources for the 3D electrode mesostructures are varied, and they include the electrode mesostructures that are obtained through the battery manufacturing digital twins that we have been introducing in the previous sections. Thus, simulating the process of electrolyte infiltration into experimentally validated 3D electrode mesostructures is an additional capability of our workflow, as shown in figure 3(A). In these regards, extending these models to LSBs should be quite straightforward after having obtained the corresponding electrode mesostructures, by accounting for all the caveats and challenges that we introduced regarding the adaptation of our models to LSBs. Of special importance for the case of LSBs are the abovementioned hydrophobicity of the conductive carbon supports, the microporosity and the sulfur loading of the C/S composites, and the initial composition of the electrolyte. In the LBM simulations, these properties manifest themselves in terms of higher contact angles, which get modulated by the carbon to sulfur surface ratios which are in contact with the electrolyte, the electrolyte viscosities and densities which highly depend on the electrolyte concentration, and the effective permeability of the C/S particles due to their microporosity. The mesostructural heterogeneities formed by differences in particle size and shapes will also be important as explained earlier, where the disposition of the C/S particles with respect to the electrolyte infiltration direction will highly affect the pore saturation dynamics.

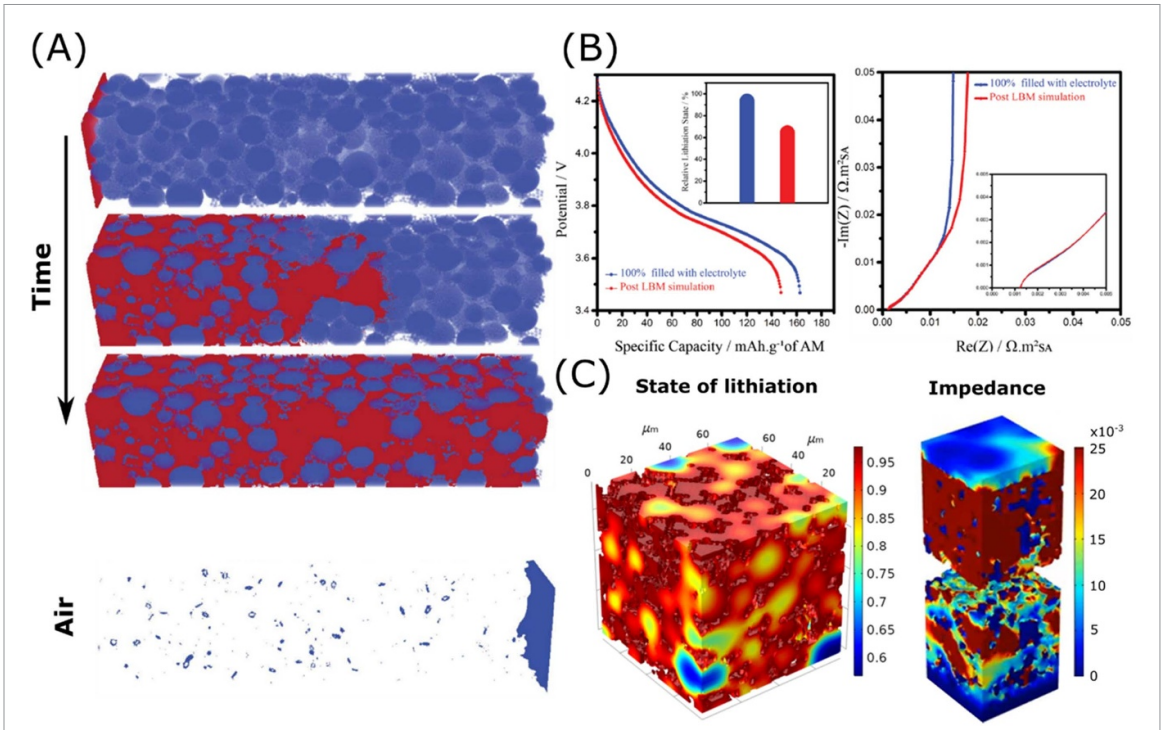

Figure 3. (A) Process of electrolyte infiltration on a CGMD model for a porous electrode. In blue the AM particles, in red the electrolyte. Trapped air is represented in blue in the bottom. Reprinted from [102], Copyright (2021), with permission from Elsevier. (B) Galvanostatic discharge curves (left) and electrochemical impedance spectra (right) of the electrodes, assuming fully wetting conditions (blue) and resolving for the explicit electrolyte distribution after LBM simulations (red). (C) 3D maps of the state of lithiation (left) and the impedance (right) of model mesostructures for LIBs, the heterogeneities are seen by the uneven distribution of colors. Reprinted from [108], Copyright (2020), with permission from Elsevier.

Additionally, in order to extend the discussion into some further capabilities of the LBM model that could be of potential interest for LSBs, we note that, within the LBM model, it is possible to include reactive flow simulations [103, 104]. Concretely, the LBM is not only useful for analyzing the permeability of porous materials and the process of electrolyte infiltration itself, but it could also be used to simulate the operation of an LSB electrode. Therefore, it could be possible to simultaneously simulate porous flow and PS dissolution/precipitation processes, where the fluid properties dynamically change with the concentration of dissolved PSs. These dynamic changes would, in turn, affect the gas–liquid and solid-liquid interactions, through density ratio, contact angle, and viscosity changes; allowing us to analyze the effects of deteriorated electrolyte wettability, such as lowered active ('wet') surface areas or electrolyte displacement effects, which are important, specially under low E/S ratio conditions. Additionally, sulfur suffers from a volume expansion of around 70% during reduction [105], which poses hard challenges for the simulation of dynamically changing meshes within the LBM framework, where newly precipitated Li_2S displaces the electrolyte. This is even more challenging because, at the mesoscale, explicitly accounting for the microporosity of the C/S composites is prohibitive in terms of computational costs. Thus, while it could be possible to identify the precipitation centers in the outer surface of the C/S composite particles, i.e. the mesoporosity of the electrode, it is not feasible to do so in the inner microporosity of the particles, and some coupling with homogenized models would be necessary.

All in all, we think that the LBM is worth exploring for simulating the process of electrolyte infiltration into LSB electrodes. While the model is straightforwardly extended to LSBs for its most simple functionality [102], still many challenges arise regarding the solution mediated reactions of PSs and precipitation of discharge products. Thus, building clever models that overcome the abovementioned problems is still desirable to exploit the full capabilities of the LBM in LSBs.

2.5. Electrochemical modeling

The mesostructures that are obtained at the end of the presented manufacturing simulation steps, i.e. drying simulations (uncalendered electrodes) [58], calendering simulations (calendered electrodes) [43], and electrolyte filling simulations (wetted electrodes) [102], are all subject to be used in 3D-resolved models in order to assess their electrochemical performance. In the case of LIBs, as shown in figure 3(B), our workflow allows us to make comparative studies where the outputted electrode mesostructures are analyzed in terms of

galvanostatic discharge/charge or electrochemical impedance spectroscopy (EIS). This allows linking the manufacturing conditions and the textural properties of the resulting mesostructures with their electrochemical performance. These models are built by defining partial differential equations (PDEs) that describe the physical processes that occur in the AM, CBD, and electrolyte phases, within the LIB porous electrodes, under different operation conditions (e.g. C-rate), by adapting the so-called Newman model [106, 107] to 3D. Concretely, the PDEs are solved on a meshed representation of the 3D electrode mesostructures, that are obtained with the manufacturing simulations, using the finite element method (FEM).

A distinguishing factor of the workflow is that, as a result of explicitly following the particle trajectories upon the manufacturing simulations, and therefore resolving for the spatial location of each of the constituent electrode phases, their individual effect on the electrochemistry of the system is perfectly distinguishable, since it allows assigning different physics to the different electrode materials in 3D (figure 3(C)). Therefore, one can, for example, investigate the impact of the spatial location of the CBD phase on the heterogeneity of the electrochemical processes. For instance, it has been shown that large heterogeneities form when the CBD phase is blocking towards the diffusion of Li^+ ions, leading to high polarization regions and poor specific capacities. On the contrary, highly porous CBD leads to smaller Li^+ concentration gradients, thus improving specific capacities and lowering polarizations [109]. Other works have shown that heterogeneities in particle- and pore-size distributions, cause the underutilization of the AM particles, thus lowering capacities and reducing power densities [110]. Additionally, rational designs have been proposed, such as graded electrodes, where particle size distributions or electrode porosities vary along the thickness of the electrodes, leading to improved rate capabilities without sacrificing specific energy densities [111]. Additionally, the spatial heterogeneities of the electrodes can also be analyzed in terms of their impedance response, as shown in figure 3(C). For this, symmetric cell simulations can be set up, mimicking their experimental analogues [112], and allowing to obtain electrode tortuosity factors [113, 114]. Therefore, a 3D-resolved EIS model has been proposed by us, showing that the electronic and ionic impedances are highly heterogeneous, and depend on the local disposition of the electrode materials [108]. Such models provide additional tools for the analysis and rational design of electrode mesostructures with improved performance. Lastly, we note that the formation of the SEI has been also predicted to be highly dependent on the heterogeneous distribution of the CBD and the different AM particle shapes. This 3D-resolved model is able to simulate heterogeneous SEI thickness distributions as a function of the mesostructural properties of the electrodes [115].

All these studies make the clear point that the heterogeneities of the electrochemical response of LIB cathodes, and anodes, highly depend on the spatial distribution of AM, CBD, and pores within the electrode mesostructures, which are directly caused by the parameters that are chosen in their manufacturing process, such as electrode formulations, slurry solid contents, drying rates, calendering degrees, electrolyte properties, etc. Indeed, electrochemical simulations have shown how manufacturing parameters such as, electrode formulations [116], calendering degrees [43], and electrolyte properties [102], alter the electrochemical performance of the corresponding electrodes. Therefore, we highlight the importance of having well parameterized and experimentally validated digital twins of the battery manufacturing process, which can explore these complex parameter spaces by digitally screening different manufacturing conditions in order to obtain the most optimal ones, thus bypassing costly experimental trial and error approaches. However, improvements are still required to obtain truly accurate models across different chemistries. For instance, most of the abovementioned models are implemented for NMC electrodes, which are well characterized, and where the Newman model, with simple Butler-Volmer (BV) reactions and Fickian solid diffusion, appears to be well suited given its solid solution reaction mechanism. However, this is not necessarily the case for every battery material. For instance, lithium-iron phosphate shows a phase separating behavior, thus Fickian solid diffusion with a constant solid diffusion coefficient is no longer a good approximation, and Allen-Cahn or Cahn-Hilliard approaches should be implemented, which are costly in terms of computational efficiency [117–120]. Additionally, the phenomenological BV reactions are shown to not be precise enough to simulate the observed inter-particle 'fictitious' phase separation behavior of NMC electrodes, under high-rate charge operation, where, auto-catalytic reactions are shown to drive the heterogeneous lithiation states of the AM particles [121].

In the case of LSBs, 3D electrochemical simulations could also be a viable tool to analyze the effect of mesostructural heterogeneities on the dissolution of sulfur, production of lithium PSs and growth of Li_2S precipitates, which will be a function of the heterogeneously distributed C/S particles and the corresponding conductive additives and binder. This is because the materials distribution within the electrodes will control the electronic and ionic current lines. However, the challenges and caveats for the accurate 3D modeling of LSBs based on FEM simulations are, for the most part, similar to the ones we already introduced for the electrochemical reactions that are included in the LBM approach. For example, moving boundary problems,

where solid Li_2S precipitates grow and displace the neighboring electrolyte, and the subsequent electrode volume expansion, are really challenging for FEM simulations, especially in 3D, involving dynamically moving meshes that respond sulfur lithiation states, electrolyte concentration gradients, etc. Liu *et al* captured the 3D mesostructural changes of volume changing Si/Graphite composite electrodes as a function of the lithiation state of the AM components [44]. However, the electrochemical model itself was still resolved in a fixed mesh, where displacement fields due to elastic deformations were calculated as a function of the particle lithiation states. Additionally, the electrolyte was approximated as a 'freely deforming' phase, which may not be the case with LSBs, where PS dissolution leads to highly viscous electrolytes that offer higher resistances to deformation. Still, such models could work as a first approximation to a fully consistent 3D FEM model for an LSB electrode. All in all, we believe that, while FEM based models are worth exploring, the solution to mesoscopic 3D electrochemical models for LSBs, will likely involve the implementation of reactive LBM models, or a coupling of both FEM and LBM. This is due to its capabilities to simultaneously account for meso- and micro-scale physical interactions, and its suitability for multiphase flow simulations, where fluid-fluid or fluid-gas 'moving' boundaries are already simulated within a fixed mesh. Still, as stated in the previous section, the shrinking of the elemental sulfur (on discharge), or the formation of Li_2S precipitates that displace the electrolyte, requires finding new ways in which all these effects are included within dynamically changing structures.

2.6. Opportunities for ML

The processing steps that we mentioned above, along with many others where a digital twin has yet to be developed (figure 1(A)) [23], comprise a battery manufacturing chain that calls for finding the optimal fabrication parameters on a complex, correlated, and often competing, parameter space. These fabrication parameters, such as the electrode materials selection, slurry solid content, mixing times and speeds, coating speeds, comma gaps, drying temperatures, calendering pressures, cell architecture design, wetting protocols, formation protocols, etc [40], are strongly correlated, and the lack of fundamental understanding about such correlations converts the battery manufacturing optimization in a 'needle in a haystack' problem. In fact, the intrinsic nature of such trial-and-error approaches is the '*a priori*' random generation of data points that are then analyzed and studied by an expert eye to inform on the experimental decision making. This classic approach has worked wonders historically. However, the increasing battery research community and the ever-increasing data production rate, makes it almost impossible for a human expert to keep track of all the parameters and hidden, often non-linear, correlations that lie beneath all the experimental or simulation data. In a previous section, we have claimed that physical based models offer opportunities to inform experimental trial and error approaches, that allow saving time and costs. While true, due to current hardware limitations and the sheer amount of data and parameters that must be considered, systematic battery manufacturing studies based on physical models are still too expensive to carry out. Thus, as pointed out by us [122], developing data-driven approaches, where trustable, and verifiable, experimental and simulation data, is systematically stored and analyzed through ML algorithms, becomes key in order to find trends and correlations where a human expert eye could not, which can hopefully accelerate the battery manufacturing optimization process (figure 4). However, creating good protocols and standards for data acquisition and storage is a colossal task that requires the cooperation of all the academic and industrial agents in the battery development field.

Surprisingly, the first work that addresses the LIB manufacturing process through ML methods at a prototyping scale is quite recent. Cunha *et al* [123], from our group, used a supervised ML model to predict the influence of the slurry viscosity, solid content, and formulation, on the final loadings and porosities of the electrodes upon drying. In particular, they showed that support vector machines (SVMs) provide quick, phase diagram-like, feedback on the influence of all the above-mentioned manufacturing parameters on electrode porosities and loadings, which might result really useful for engineers and technicians that want fast guidelines for slurry processing. After this, many other researchers have utilized ML methods to inform experimental designs for LIBs. Chen *et al* [124], in collaboration with our group, used similar methods to decipher parameter interdependencies on the fabrication of highly conductive and homogeneous solid-state electrolyte films. Similarly, Duquesnoy *et al* [125] from our group used the supervised Gaussian Naives Bayes (GNB) technique in order to assess the probability of casting homogeneous LIB electrodes depending on AM percentages, comma gaps, and slurry solid contents. Those works describe the use of supervised ML algorithms using experimental datasets as an input, however the extent of the applicability of ML is not limited to only one type of data. Indeed, Duquesnoy *et al* [126], from our group, also reported a combined approach, where scarce experimental data points, containing initial porosities before calendering, AM contents, and calendering roll gaps, were first fitted to output the electrode porosities after calendering. Then, using this polynomial fitting, *in silico* stochastically generated 3D electrode mesostructures were used to obtain further mesostructural information such as tortuosity factors, surface areas of contact of AM and

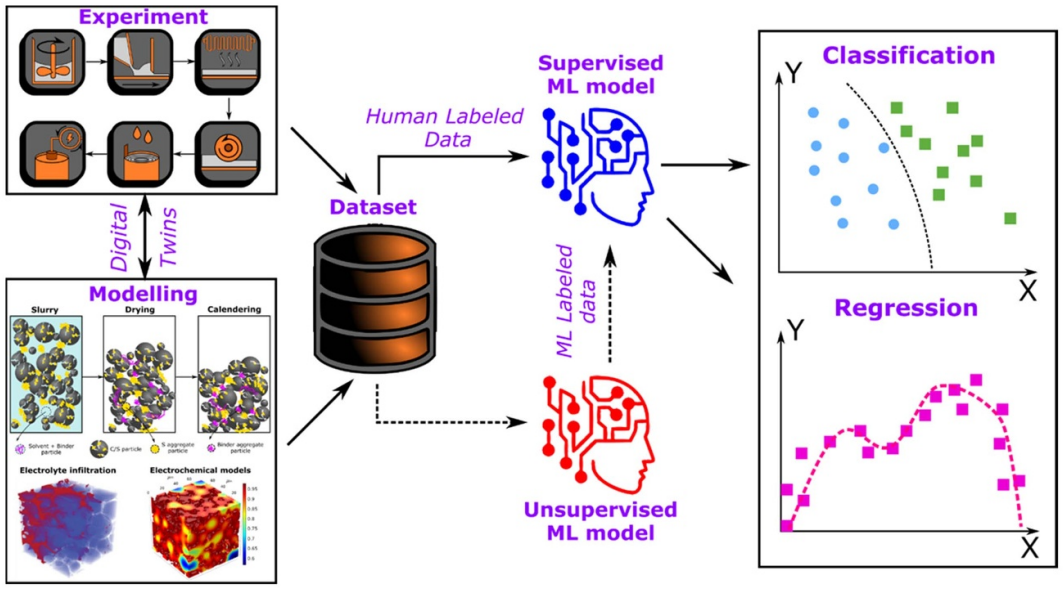

Figure 4. General workflow for the application of ML (supervised/unsupervised) models for classification and regression purposes. From left to right, the data generated by the battery manufacturing experiments and models is saved in datasets, which are then used to train supervised ML models for classification and regression. Unsupervised ML models are marked in dotted arrows, representing their potential use for data labeling without human intervention.

CBD with the CC, and the AM-electrolyte surface areas. The supervised regression ML model was based on the sure independent screening and sparsifying operator (SISSO) [127]. This ML model, which is particularly suited to obtain descriptors in small datasets, allowed to obtain highly accurate predictions on the mesostructural properties of the manufactured electrodes based on fabrication parameters. All these works deal with supervised learning algorithms, however unsupervised algorithms have also proved to be useful. Primo *et al* from our group [128] showed that a combination of statistical covariance analysis, through the analysis of covariance (ANCOVA) method, and a combination of principal components analysis (PCA) and k-means clustering, was useful in deciphering the impact of calendering parameters (calendering pressure, line speed and temperature) onto the final electrode properties, such as porosities, mechanical properties, electronic conductivities, volumetric capacities, etc.

Apart from the applications of ML models to predict electrode properties from experimental parameters or physical simulations, ML models could also be used to improve the performance of the physical simulations themselves. This has been a long subject of discussion in the material science community, where ML trained FFs have been used in order to be able to run more efficient classical MD simulations with an accuracy similar to that obtainable by computationally demanding *ab initio* molecular dynamics [129]. From the battery manufacturing simulations perspective, ML models have been effectively used to accelerate costly LBM simulations for electrolyte infiltration into porous electrodes. A combination of pore-network models and training data coming from LBM simulations, was used to predict electrolyte saturation levels in porous electrodes using multilayer perceptrons (MLPs), at a fraction of the computational cost (few seconds) when compared to LBM simulations (days) [130].

The abovementioned ML models, which predict relationships between manufacturing conditions and electrode properties, could also be nicely adapted to LSBs, of course considering fabrication and cell design considerations that are specific to LSBs [25, 131]. Indeed, as far as we know, first attempts to apply ML models to the design parameters of LSBs were performed by Kilic *et al* [132], where they used association rule mining techniques to extract and analyze data for 1660 cells reported in the literature. The resulting data analysis shows the materials and design factors that are critical to obtain high peak discharge capacities and cycle lifes. Their conclusions show that using sulfur encapsulating carbon materials, here referred to as C/S composites, is critical for the performance of LSBs. Other considerations such as binder-types, electrolyte materials that allow operation at low E/S ratios, and the use of interlayers have been found to improve the overall performance of LSBs. Still, ML models that explicitly relate manufacturing parameters of LSBs and their electrode properties are needed, in order to correlate the critical metrics for LSBs, such as having uniform coatings that allow for high energy density thick electrodes, low E/S ratios, low E/C ratios, optimized tortuosity electrodes that prevent the PS shuttle effect, etc, with the manufacturing process parameters described above.

Lastly, we note that most of the ML models that we have described work with fairly small datasets, which are generated specifically for the purposes of the studies. However, the reusability of such datasets is often limited by the lack of standards and generality [122]. This 'atomized' use of ML models is far from ideal, as it lacks interoperability and misses on the potential of having truly extensive datasets, that provide accurate ML predictions for the battery properties of interest. Text mining has the potential to alleviate this issue, by scraping through the hundreds of thousands of articles reporting battery properties and manufacturing conditions, and by 'curating' the data into comprehensive, general, and ready to use databases. Indeed, such approaches have been successfully applied to the field of materials science [133, 134]. However, El-Bousidy *et al* from our group [135] showed, through similar text mining techniques, that LIB research articles show a general lack of consistent reporting of electrode properties, such as thicknesses, porosities, loadings, electrolyte volumes or surface areas. This poses serious problems for the completeness of the reported data, which hampers the correct prediction of battery properties through ML models, and brings out yet another example of the reproducibility crisis common to various scientific disciplines [136]. Therefore, deeper assessments of reporting practices in the field of LSBs will also be necessary to further advance the knowledge in the field, and to allow researchers to reproduce literature works. In general, we believe that encouraging scientists to think about standard reporting practices without burdening the scientific discovery process, is a must in the battery manufacturing field, and this includes LSBs. In these lines, several battery related journals have proposed checklists, or have started to request standardized battery data reporting [137–139].

3. Conclusions

This work aims at identifying the different challenges and opportunities that we think could be interesting to study regarding the implementation of manufacturing digital twins for LSBs. We have identified six areas of interest, where LIB manufacturing simulations could be adapted to LSBs via physics-based slurry, drying, calendering, electrolyte infiltration, electrochemical performance, and ML models. Slurry models can be straightforwardly adapted to LSBs, where μm-sized C/S composite beads are simulated with CGMD, and where the experimental validation of the slurry model focuses on its rheological properties (viscosity vs shear-rate curves) and its density. Similarly, the drying simulations, where the first uncalendered electrode mesostructures are obtained, could be directly adapted to LSBs, considering a few differences: (a) the typically higher amount of carbon and binder additives that are included mixed with the C/S composites, which may change the behavior of the migrating binder, when compared to LIB electrodes, with lower additive contents, and (b) the potential loss of elemental sulfur as a result of drying temperatures. Calendering models, simulated through DEM, and experimentally validated against final electrode porosities and compaction curves, could also be straightforwardly adapted to LSBs. However, at this stage, many challenges start to manifest due to the intrinsic differences between the mechanical properties of C/S composite and AM particles (such as NMC) used in LIBs. The softer C/S particles may be subject to large deformations upon compressive loads, and thus the spherical particle approximation would no longer be valid. Therefore, there is a need to account for the realistic shape changes of C/S particles, for example, through multi-sphere approaches. Equivalently, this multi-sphere approach may also be used to simulate C/S particles of arbitrary shapes (fibers, platelets, etc) for the previously mentioned slurry and drying simulations. Continuing with the manufacturing process, the electrolyte filling simulations are introduced. We note that the LBM is the go-to simulation tool when trying to analyze multi-phase fluid flow in porous electrodes, and it could be readily applied to LSBs. Nevertheless, further exploiting LBM simulations for the specific purposes of LSBs, requires building new models that account for sulfur reduction and precipitation reactions, dynamic changes in the electrolyte viscosity and density due to PS dissolution, electrode volume expansion upon sulfur reduction, and electrolyte displacement phenomena, among others. Then, the viability of other more classical electrochemical modeling approaches through FEM simulations is assessed. Although highly useful and studied for LIBs, developing full 3D-resolved electrochemical models for LSBs requires considering many challenges, similar to those presented for LBM simulations, but without the intrinsic benefits that LBM simulations offer to simulate multiphase fluid flow. Lastly, we discussed the opportunities for applying ML techniques to uncover complex correlations between LSB manufacturing parameters and electrode properties. Concretely, we discuss that several ML models exist that address this issue for LIBs, which also have a straightforward application for LSBs, such as the supervised SVM, GNB, SISSO and MLP methods, or unsupervised PCA and k-means clustering methods. Furthermore, we briefly discuss text mining as a potential tool to obtain well curated big datasets from the literature, for their applications in ML, for both LIBs and LSBs. We conclude that, while being an interesting approach, there is a general lack of consistency in the reported battery properties and manufacturing conditions, which calls for standardizing reporting practices amongst battery scientist, which apply equally to LIBs and LSBs.

Summing up, as the field of LSBs keeps advancing with more sophisticated and precise experimental methods, there is a call for more complex and realistic models. Specifically, modeling the manufacturing processes of LSBs, and connecting those processes to the mesostructural properties of the resulting electrodes, has the potential to be an invaluable tool for rational design and understanding of the relevant processes that happen inside this fascinating system. Mesoscale models in 3D have the strength of explicitly defining the structure of porous electrodes, and therefore have the unique ability of pin-pointing potential failure points in the existing mesostructures, allowing researchers to come up with new electrode architectures that circumvent these issues. The trade-off lies in the increased computational costs related to the explicit definition of the mesostructures and the complex multi-physics phenomena that take place within. However, the growing computing power of high performance computers (HPCs) and the application of efficient and low-cost ML methods are allowing for a more generalized use of such 3D mesoscale models.

Data availability statement

No new data were created or analyzed in this study.

Acknowledgments

A A F, acknowledges the European Union's Horizon 2020 research and innovation programme for the funding support through the European Research Council (Grant Agreement 772873, 'ARTISTIC' project). A A F and O A acknowledge funding from the European Union's Horizon 2020 research and innovation program under Grant Agreement No. 957189 (BIG-MAP). BATTERY 2030+ initiative under Grant Agreement No. 957213 is also acknowledged. A A F acknowledges Institut Universitaire de France for the support. A A F and O A acknowledge the funding from Conseil régional des Hauts de France and the Université Picardie Jules Verne under project name (OPERANDO).

ORCID iD

Alejandro A Franco https://orcid.org/0000-0001-7362-7849

References

[1] Opitz A, Badami P, Shen L, Vignarooban K and Kannan A M 2017 Can Li-ion batteries be the panacea for automotive applications? *Renew. Sustain. Energy Rev.* **68** 685–92
[2] Sun Y-K 2020 Promising all-solid-state batteries for future electric vehicles *ACS Energy Lett.* **5** 3221–3
[3] Janek J and Zeier W G 2016 A solid future for battery development *Nat. Energy* **1** 16141
[4] Manthiram A 2017 An outlook on lithium ion battery technology *ACS Central Sci.* **3** 1063–9
[5] Choi J W and Aurbach D 2016 Promise and reality of post-lithium-ion batteries with high energy densities *Nat. Rev. Mater.* **1** 16013
[6] Bruce P G, Freunberger S A, Hardwick L J and Tarascon J M 2012 Li–O_2 and Li–S batteries with high energy storage *Nat. Mater.* **11** 19–29
[7] Manthiram A, Fu Y, Chung S H, Zu C and Su Y S 2014 Rechargeable lithium-sulfur batteries *Chem. Rev.* **114** 11751–87
[8] Lv D *et al* 2015 High energy density lithium-sulfur batteries: challenges of thick sulfur cathodes *Adv. Energy Mater.* **5** 1–8
[9] Mikhaylik Y V and Akridge J R 2004 Polysulfide shuttle study in the Li/S battery system *J. Electrochem. Soc.* **151** A1969
[10] Diao Y, Xie K, Xiong S and Hong X 2013 Shuttle phenomenon-the irreversible oxidation mechanism of sulfur active material in Li-S battery *J. Power Sources* **235** 181–6
[11] Wild M, O'Neill L, Zhang T, Purkayastha R, Minton G, Marinescu M and Offer G J 2015 Lithium sulfur batteries, a mechanistic review *Energy Environ. Sci.* **8** 3477–94
[12] Al-Mahmoud S M, Dibden J W, Owen J R, Denuault G and Garcia-Araez N 2016 A simple, experiment-based model of the initial self-discharge of lithium-sulphur batteries *J. Power Sources* **306** 323–8
[13] Ji X, Lee K T and Nazar L F 2009 A highly ordered nanostructured carbon–sulphur cathode for lithium–sulphur batteries *Nat. Mater.* **8** 500–6
[14] Borchardt L, Oschatz M and Kaskel S 2016 Carbon materials for lithium sulfur batteries—ten critical questions *Chem. Eur. J.* **22** 7324–51
[15] Li G *et al* 2021 Carbon foam fibers with a concentric tube-core/three-dimensional nanosheet-sheath structure for high-performance lithium-sulfur batteries *ChemElectroChem* **8** 873–9
[16] Li N, Meng T, Ma L, Zhang H, Yao J, Xu M, Li C M and Jiang J 2020 Curtailing carbon usage with addition of functionalized $NiFe_2O_4$ quantum dots: toward more practical S cathodes for Li–S cells *Nano-Micro Lett.* **12** 145
[17] Chen J *et al* 2016 Restricting the solubility of polysulfides in Li-S batteries via electrolyte salt selection *Adv. Energy Mater.* **6** 1600160
[18] Shin E S, Kim K, Oh S H and Cho W I 2013 Polysulfide dissolution control: the common ion effect *Chem. Commun.* **49** 2004–6
[19] Gupta A and Sivaram S 2019 Separator membranes for lithium–sulfur batteries: design principles, structure, and performance *Energy Technol.* **7** 1800819
[20] Rana M, Li M, Huang X, Luo B, Gentle I and Knibbe R 2019 Recent advances in separators to mitigate technical challenges associated with re-chargeable lithium sulfur batteries *J. Mater. Chem.* A **7** 6596–615

[21] Cheng X B, Zhang R, Zhao C Z and Zhang Q 2017 Toward safe lithium metal anode in rechargeable batteries: a review *Chem. Rev.* **117** 10403–73
[22] Zhang H, Eshetu G G, Judez X, Li C, Rodriguez-Martínez L M and Armand M 2018 Electrolyte additives for lithium metal anodes and rechargeable lithium metal batteries: progress and perspectives *Angew. Chem., Int. Ed.* **57** 15002–27
[23] Duffner F, Kronemeyer N, Tübke J, Leker J, Winter M and Schmuch R 2021 Post-lithium-ion battery cell production and its compatibility with lithium-ion cell production infrastructure *Nat. Energy* **6** 123–34
[24] Kang N, Lin Y, Yang L, Lu D, Xiao J, Qi Y and Cai M 2019 Cathode porosity is a missing key parameter to optimize lithium-sulfur battery energy density *Nat. Commun.* **10** 1–10
[25] Bhargav A, He J, Gupta A and Manthiram A 2020 Lithium-sulfur batteries: attaining the critical metrics *Joule* **4** 285–91
[26] Andersen A, Rajput N N, Han K S, Pan H, Govind N, Persson K A, Mueller K T and Murugesan V 2019 Structure and dynamics of polysulfide clusters in a nonaqueous solvent mixture of 1,3-dioxolane and 1,2-dimethoxyethane *Chem. Mater.* **31** 2308–19
[27] Rajput N N, Murugesan V, Shin Y, Han K S, Lau K C, Chen J, Liu J, Curtiss L A, Mueller K T and Persson K A 2017 Elucidating the solvation structure and dynamics of lithium polysulfides resulting from competitive salt and solvent interactions *Chem. Mater.* **29** 3375–9
[28] Shen J, Wang Z, Xu X, Liu Z, Zhang D, Li F, Li Y, Zeng L and Liu J 2021 Surface/interface structure and chemistry of lithium–sulfur batteries: from density functional theory calculations' perspective *Adv. Energy Sustain. Res.* **2** 2100007
[29] Ghaznavi M and Chen P 2014 Sensitivity analysis of a mathematical model of lithium-sulfur cells: part II: precipitation reaction kinetics and sulfur content *J. Power Sources* **257** 402–11
[30] Ghaznavi M and Chen P 2014 Sensitivity analysis of a mathematical model of lithium-sulfur cells part I: applied discharge current and cathode conductivity *J. Power Sources* **257** 394–401
[31] Ghaznavi M and Chen P 2014 Analysis of a mathematical model of lithium-sulfur cells part III: electrochemical reaction kinetics, transport properties and charging *Electrochim. Acta* **137** 575–85
[32] Thangavel V, Mastouri A, Guéry C, Morcrette M and Franco A A 2021 Understanding the reaction steps involving polysulfides in 1 M LiTFSI in TEGDME:DOL using cyclic voltammetry experiments and modelling *Batteries Supercaps* **4** 152–62
[33] Thangavel V, Xue K-H, Mammeri Y, Quiroga M, Mastouri A, Guéry C, Johansson P, Morcrette M and Franco A A 2016 A microstructurally resolved model for Li-S batteries assessing the impact of the cathode design on the discharge performance *J. Electrochem. Soc.* **163** A2817–29
[34] Danner T, Zhu G, Hofmann A F and Latz A 2015 Modeling of nano-structured cathodes for improved lithium-sulfur batteries *Electrochim. Acta* **184** 124–33
[35] Mistry A and Mukherjee P P 2017 Precipitation-microstructure interactions in the Li-sulfur battery electrode *J. Phys. Chem.* C **121** 26256–64
[36] Thangavel V, Guerrero O X, Quiroga M, Mikala A M, Rucci A and Franco A A 2020 A three dimensional kinetic Monte Carlo model for simulating the carbon/sulfur mesostructural evolutions of discharging lithium sulfur batteries *Energy Storage Mater.* **24** 472–85
[37] Perez Beltran S and Balbuena P B 2018 Formation of multilayer graphene domains with strong sulfur–carbon interaction and enhanced sulfur reduction zones for lithium–sulfur battery cathodes *ChemSusChem* **11** 1970–80
[38] Ryan E M and Mukherjee P P 2019 Mesoscale modeling in electrochemical devices—a critical perspective *Prog. Energy Combust. Sci.* **71** 118–42
[39] ARTISTIC Project (available at: www.erc-artistic.eu/) (Accessed 27 October 2021)
[40] Liu Y, Zhang R, Wang J and Wang Y 2021 Current and future lithium-ion battery manufacturing *iScience* **24** 102332
[41] Ngandjong A C, Rucci A, Maiza M, Shukla G, Vazquez-Arenas J and Franco A A 2017 Multiscale simulation platform linking lithium ion battery electrode fabrication process with performance at the cell level *J. Phys. Chem. Lett.* **8** 5966–72
[42] Lombardo T, Hoock J, Primo E, Ngandjong C, Duquesnoy M and Franco A A 2020 Accelerated optimization methods for force-field parametrization in battery electrode manufacturing modeling *Batteries Supercaps* **3** 721–30
[43] Ngandjong A C, Lombardo T, Primo E N, Chouchane M, Shodiev A, Arcelus O and Franco A A 2021 Investigating electrode calendering and its impact on electrochemical performance by means of a new discrete element method model: towards a digital twin of Li-Ion battery manufacturing *J. Power Sources* **485** 229320
[44] Liu C, Arcelus O, Lombardo T, Oularbi H and Franco A A 2021 Towards a 3D-resolved model of Si/graphite composite electrodes from manufacturing simulations *J. Power Sources* **512** 230486
[45] Bauer W and Nötzel D 2014 Rheological properties and stability of NMP based cathode slurries for lithium ion batteries *Ceram. Int.* **40** 4591–8
[46] Xu T, Song J, Gordin M L, Sohn H, Yu Z, Chen S and Wang D 2013 Mesoporous carbon-carbon nanotube-sulfur composite microspheres for high-areal-capacity lithium-sulfur battery cathodes *ACS Appl. Mater. Interfaces* **5** 11355–62
[47] Sohn H, Gordin M L, Xu T, Chen S, Lv D, Song J, Manivannan A and Wang D 2014 Porous spherical carbon/sulfur nanocomposites by aerosol-assisted synthesis: the effect of pore structure and morphology on their electrochemical performance as lithium/sulfur battery cathodes *ACS Appl. Mater. Interfaces* **6** 7596–606
[48] Zeng F, Wang A, Wang W, Jin Z and Yang Y S 2017 Strategies of constructing stable and high sulfur loading cathodes based on the blade-casting technique *J. Mater. Chem.* A **5** 12879–88
[49] Ferellec J F and McDowell G R 2010 A method to model realistic particle shape and inertia in DEM *Granular Matter* **12** 459–67
[50] Jaiser S, Friske A, Baunach M, Scharfer P and Schabel W 2017 Development of a three-stage drying profile based on characteristic drying stages for lithium-ion battery anodes *Drying Technol.* **35** 1266–75
[51] Jaiser S, Müller M, Baunach M, Bauer W, Scharfer P and Schabel W 2016 Investigation of film solidification and binder migration during drying of Li-ion battery anodes *J. Power Sources* **318** 210–9
[52] Jaiser S, Funk L, Baunach M, Scharfer P and Schabel W 2017 Experimental investigation into battery electrode surfaces: the distribution of liquid at the surface and the emptying of pores during drying *J. Colloid Interface Sci.* **494** 22–31
[53] Kumberg J, Müller M, Diehm R, Spiegel S, Wachsmann C, Bauer W, Scharfer P and Schabel W 2019 Drying of lithium-ion battery anodes for use in high-energy cells: influence of electrode thickness on drying time, adhesion, and crack formation *Energy Technol.* **7** 1900722
[54] Stein M, Mistry A and Mukherjee P P 2017 Mechanistic understanding of the role of evaporation in electrode processing *J. Electrochem. Soc.* **164** A1616–27
[55] Liu Z and Mukherjee P P 2014 Microstructure evolution in lithium-ion battery electrode processing *J. Electrochem. Soc.* **161** E3248–58

[56] Font F, Protas B, Richardson G and Foster J M 2018 Binder migration during drying of lithium-ion battery electrodes: modelling and comparison to experiment *J. Power Sources* **393** 177–85
[57] Susarla N, Ahmed S and Dees D W 2018 Modeling and analysis of solvent removal during Li-ion battery electrode drying *J. Power Sources* **378** 660–70
[58] Lombardo T, Ngandjong A C, Belhcen A and Franco A A 2021 Carbon-binder migration: a three-dimensional evaporation model for lithium ion batteries *Energy Storage Mater.* **43** 337–47
[59] Hagen M, Dörfler S, Fanz P, Berger T, Speck R, Tübke J, Althues H, Hoffmann M J, Scherr C and Kaskel S 2013 Development and costs calculation of lithium-sulfur cells with high sulfur load and binder free electrodes *J. Power Sources* **224** 260–8
[60] Hagiwara H, Suszynski W J and Francis L F 2014 A Raman spectroscopic method to find binder distribution in electrodes during drying *J. Coat. Technol. Res.* **11** 11–17
[61] Lim S, Kim S, Ahn K H and Lee S J 2015 Stress development of Li-ion battery anode slurries during the drying process *Ind. Eng. Chem. Res.* **54** 6146–55
[62] Balakumar K and Kalaiselvi N 2015 High sulfur loaded carbon aerogel cathode for lithium-sulfur batteries *RSC Adv.* **5** 34008–18
[63] Primo E N, Chouchane M, Touzin M, Vazquez P and Franco A A 2021 Understanding the calendering processability of $Li(Ni_{0.33}Mn_{0.33}Co_{0.33})O_2$-based cathodes *J. Power Sources* **488** 229361
[64] Schreiner D, Oguntke M, Günther T and Reinhart G 2019 Modelling of the calendering process of NMC-622 cathodes in battery production analyzing machine/material–process–structure correlations *Energy Technol.* **7** 1900840
[65] van Bommel A and Divigalpitiya R 2012 Effect of calendering $LiFePO_4$ electrodes *J. Electrochem. Soc.* **159** A1791–5
[66] Meyer C, Weyhe M, Haselrieder W and Kwade A 2020 Heated calendering of cathodes for lithium-ion batteries with varied carbon black and binder contents *Energy Technol.* **8** 1900175
[67] Meyer C, Bockholt H, Haselrieder W and Kwade A 2017 Characterization of the calendering process for compaction of electrodes for lithium-ion batteries *J. Mater. Process. Technol.* **249** 172–8
[68] Zheng H, Tan L, Liu G, Song X and Battaglia V S 2012 Calendering effects on the physical and electrochemical properties of $Li[Ni_{1/3}Mn_{1/3}Co_{1/3}]O_2$ cathode *J. Power Sources* **208** 52–57
[69] Srivastava I, Bolintineanu D S, Lechman J B and Roberts S A 2020 Controlling binder adhesion to impact electrode mesostructures and transport *ACS Appl. Mater. Interfaces* **12** 34919–30
[70] Stershic A J, Simunovic S and Nanda J 2015 Modeling the evolution of lithium-ion particle contact distributions using a fabric tensor approach *J. Power Sources* **297** 540–50
[71] Sangrós Giménez C, Finke B, Nowak C, Schilde C and Kwade A 2018 Structural and mechanical characterization of lithium-ion battery electrodes via DEM simulations *Adv. Powder Technol.* **29** 2312–21
[72] Sangrós Giménez C, Finke B, Schilde C, Froböse L and Kwade A 2019 Numerical simulation of the behavior of lithium-ion battery electrodes during the calendaring process via the discrete element method *Powder Technol.* **349** 1–11
[73] Sangrós Giménez C, Schilde C, Froböse L, Ivanov S and Kwade A 2020 Mechanical, electrical, and ionic behavior of lithium-ion battery electrodes via discrete element method simulations *Energy Technol.* **8** 1900180
[74] Chen Y H, Wang C W, Zhang X and Sastry A M 2010 Porous cathode optimization for lithium cells: ionic and electronic conductivity, capacity, and selection of materials *J. Power Sources* **195** 2851–62
[75] Murphy W, Soifer B T, Matthews K, El M A and Davies D K 1973 Surface charge and the contact of elastic solids *J. Phys. D: Appl. Phys.* **6** 1017
[76] de Vasconcelos L S, Xu R, Li J and Zhao K 2016 Grid indentation analysis of mechanical properties of composite electrodes in Li-ion batteries *Extreme Mech. Lett.* **9** 495–502
[77] Xu R, Sun H, de Vasconcelos L S and Zhao K 2017 Mechanical and structural degradation of $LiNi_xMn_yCo_zO_2$ cathode in Li-ion batteries: an experimental study *J. Electrochem. Soc.* **164** A3333–41
[78] Yang W *et al* 2016 Large-deformation and high-strength amorphous porous carbon nanospheres *Sci. Rep.* **6** 24187
[79] Arai Y, Daigo Y, Kojo E, Inoue R and Kogo Y 2021 Relationship between the microstructures and Young's modulus of 3D-networked porous carbon material *J. Mater. Sci.* **56** 10338–52
[80] Iizuka H, Fushitani M, Okabe T and Saito K 1999 Mechanical properties of woodceramics: a porous carbon material *J. Porous Mater.* **6** 175–84
[81] Islam M M, Ostadhossein A, Borodin O, Yeates A T, Tipton W W, Hennig R G, Kumar N and van Duin A C T 2015 ReaxFF molecular dynamics simulations on lithiated sulfur cathode materials *Phys. Chem. Chem. Phys.* **17** 3383–93
[82] Wood D L, Li J and An S J 2019 Formation challenges of lithium-ion battery manufacturing *Joule* **3** 2884–8
[83] Jeon D H 2019 Wettability in electrodes and its impact on the performance of lithium-ion batteries *Energy Storage Mater.* **18** 139–47
[84] An S J, Li J, Daniel C, Mohanty D, Nagpure S and Wood D L 2016 The state of understanding of the lithium-ion-battery graphite solid electrolyte interphase (SEI) and its relationship to formation cycling *Carbon* **105** 52–76
[85] Schilling A, Wiemers-Meyer S, Winkler V, Nowak S, Hoppe B, Heimes H H, Dröder K and Winter M 2020 Influence of separator material on infiltration rate and wetting behavior of lithium-ion batteries *Energy Technol.* **8** 1900078
[86] Davoodabadi A, Li J, Liang Y, Wang R, Zhou H, Wood D L, Singler T J and Jin C 2018 Characterization of surface free energy of composite electrodes for lithium-ion batteries *J. Electrochem. Soc.* **165** A2493–501
[87] Schilling A, Gümbel P, Möller M, Kalkan F, Dietrich F and Dröder K 2019 X-ray based visualization of the electrolyte filling process of lithium ion batteries *J. Electrochem. Soc.* **166** A5163–7
[88] Weydanz W J, Reisenweber H, Gottschalk A, Schulz M, Knoche T, Reinhart G, Masuch M, Franke J and Gilles R 2018 Visualization of electrolyte filling process and influence of vacuum during filling for hard case prismatic lithium ion cells by neutron imaging to optimize the production process *J. Power Sources* **380** 126–34
[89] Knoche T, Zinth V, Schulz M, Schnell J, Gilles R and Reinhart G 2016 *In situ* visualization of the electrolyte solvent filling process by neutron radiography *J. Power Sources* **331** 267–76
[90] Peter C, Nikolowski K, Reuber S, Wolter M and Michaelis A 2020 Chronoamperometry as an electrochemical *in situ* approach to investigate the electrolyte wetting process of lithium-ion cells *J. Appl. Electrochem.* **50** 295–309
[91] Davoodabadi A, Li J, Zhou H, Wood D L, Singler T J and Jin C 2019 Effect of calendering and temperature on electrolyte wetting in lithium-ion battery electrodes *J. Energy Storage* **26** 101034
[92] Davoodabadi A, Li J, Liang Y, Wood D L, Singler T J and Jin C 2019 Analysis of electrolyte imbibition through lithium-ion battery electrodes *J. Power Sources* **424** 193–203

[93] Jin Q, Qi X, Yang F, Jiang R, Xie Y, Qie L and Huang Y 2021 The failure mechanism of lithium-sulfur batteries under lean-ether-electrolyte conditions *Energy Storage Mater.* **38** 255–61
[94] Hwang J-Y, Kim H M and Sun Y-K 2018 Controlling the wettability between freestanding electrode and electrolyte for high energy density lithium-sulfur batteries *J. Electrochem. Soc.* **165** A5006–13
[95] Niu X D, Hyodo S A, Munekata T and Suga K 2007 Kinetic lattice Boltzmann method for microscale gas flows: issues on boundary condition, relaxation time, and regularization *Phys. Rev.* E **76** 036711
[96] Chen L, Kang Q, Mu Y, He Y L and Tao W Q 2014 A critical review of the pseudopotential multiphase lattice Boltzmann model: methods and applications *Int. J. Heat Mass Transfer* **76** 210–36
[97] Pan C, Hilpert M and Miller C T 2004 Lattice-Boltzmann simulation of two-phase flow in porous media *Water Resour. Res.* **40** W01501
[98] Lee S G, Jeon D H, Kim B M, Kang J H and Kim C-J 2013 Lattice Boltzmann simulation for electrolyte transport in porous electrode of lithium ion batteries *J. Electrochem. Soc.* **160** H258–65
[99] Lee S G and Jeon D H 2014 Effect of electrode compression on the wettability of lithium-ion batteries *J. Power Sources* **265** 363–9
[100] Mohammadian S K and Zhang Y 2020 Thermal management of Li-ion batteries by embedding microgrooves inside the electrodes: a thermal lattice Boltzmann method study *J. Heat Transfer* **142** 052902
[101] Jeong H, Lim S-J, Chakravarthy S, Kim K H, Lee J, Heo J S and Park H 2020 Three-dimensional cathode with periodically aligned microchannels for improving volumetric energy density of lithium-ion batteries *J. Power Sources* **451** 227764
[102] Shodiev A, Primo E, Arcelus O, Chouchane M, Osenberg M, Hilger A, Manke I, Li J and Franco A A 2021 Insight on electrolyte infiltration of lithium ion battery electrodes by means of a new three-dimensional-resolved lattice Boltzmann model *Energy Storage Mater.* **38** 80–92
[103] Lei T and Luo K H 2021 Lattice Boltzmann simulation of multicomponent porous media flows with chemical reaction *Front. Phys.* **9** 715791
[104] Zhang D, Forner-Cuenca A, Taiwo O O, Yufit V, Brushett F R, Brandon N P, Gu S and Cai Q 2020 Understanding the role of the porous electrode microstructure in redox flow battery performance using an experimentally validated 3D pore-scale lattice Boltzmann model *J. Power Sources* **447** 227249
[105] Cheng L, Curtiss L A, Zavadil K R, Gewirth A A, Shao Y and Gallagher K G 2016 Sparingly solvating electrolytes for high energy density lithium-sulfur batteries *ACS Energy Lett.* **1** 503–9
[106] Fuller T F, Doyle M and Newman J 1994 Simulation and optimization of the dual lithium ion insertion cell *J. Electrochem. Soc.* **141** 1–10
[107] Doyle M, Fuller T F and Newman J 1993 Modeling of galvanostatic charge and discharge of the lithium/polymer/insertion cell *J. Electrochem. Soc.* **140** 1526–33
[108] Shodiev A, Primo E N, Chouchane M, Lombardo T, Ngandjong A C, Rucci A and Franco A A 2020 4D-resolved physical model for electrochemical impedance spectroscopy of $Li(Ni_{1-x-y}Mn_xCo_y)O_2$-based cathodes in symmetric cells: consequences in tortuosity calculations *J. Power Sources* **454** 227871
[109] Chouchane M, Rucci A, Lombardo T, Ngandjong A C and Franco A A 2019 Lithium ion battery electrodes predicted from manufacturing simulations: assessing the impact of the carbon-binder spatial location on the electrochemical performance *J. Power Sources* **444** 227285
[110] Lu X *et al* 2020 3D microstructure design of lithium-ion battery electrodes assisted by x-ray nano-computed tomography and modelling *Nat. Commun.* **11** 2079
[111] Lu X *et al* 2021 Multi-length scale microstructural design of lithium-ion battery electrodes for improved discharge rate performance *Energy Environ. Sci.* **14** 5929–46
[112] Ogihara N, Kawauchi S, Okuda C, Itou Y, Takeuchi Y and Ukyo Y 2012 Theoretical and experimental analysis of porous electrodes for lithium-ion batteries by electrochemical impedance spectroscopy using a symmetric cell *J. Electrochem. Soc.* **159** A1034–9
[113] Nguyen T T, Demortière A, Fleutot B, Delobel B, Delacourt C and Cooper S J 2020 The electrode tortuosity factor: why the conventional tortuosity factor is not well suited for quantifying transport in porous Li-ion battery electrodes and what to use instead *npj Comput. Mater.* **6** 123
[114] Malifarge S, Delobel B and Delacourt C 2017 Determination of tortuosity using impedance spectra analysis of symmetric cell *J. Electrochem. Soc.* **164** E3329–34
[115] Chouchane M, Arcelus O and Franco A A 2021 Heterogeneous solid-electrolyte interphase in graphite electrodes assessed by 4D-resolved computational simulations *Batteries Supercaps* **4** 1457–63
[116] Rucci A, Ngandjong A C, Primo E N, Maiza M and Franco A A 2019 Tracking variabilities in the simulation of lithium ion battery electrode fabrication and its impact on electrochemical performance *Electrochim. Acta* **312** 168–78
[117] Ferguson T R and Bazant M Z 2012 Nonequilibrium thermodynamics of porous electrodes *J. Electrochem. Soc.* **159** A1967–85
[118] Smith R B and Bazant M Z 2017 Multiphase porous electrode theory *J. Electrochem. Soc.* **164** E3291–310
[119] Bazant M Z 2013 Theory of chemical kinetics and charge transfer based on nonequilibrium thermodynamics *Acc. Chem. Res.* **46** 1144–60
[120] Li Y *et al* 2014 Current-induced transition from particle-by-particle to concurrent intercalation in phase-separating battery electrodes *Nat. Mater.* **13** 1149–56
[121] Park J *et al* 2021 Fictitious phase separation in Li layered oxides driven by electro-autocatalysis *Nat. Mater.* **20** 991–9
[122] Lombardo T *et al* 2021 Artificial intelligence applied to battery research: hype or reality? *Chem. Rev.* (https://doi.org/10.1021/acs.chemrev.1c00108)
[123] Cunha R P, Lombardo T, Primo E N and Franco A A 2020 Artificial intelligence Investigation of NMC cathode manufacturing parameters interdependencies *Batteries Supercaps* **3** 60–67
[124] Chen Y T, Duquesnoy M, Tan D H S, Doux J M, Yang H, Deysher G, Ridley P, Franco A A, Meng Y S and Chen Z 2021 Fabrication of high-quality thin solid-state electrolyte films assisted by machine learning *ACS Energy Lett.* **6** 1639–48
[125] Duquesnoy M, Boyano I, Ganborena L, Cereijo P, Ayerbe E and Franco A A 2021 Machine learning-based assessment of the impact of the manufacturing process on battery electrode heterogeneity *Energy* AI **5** 100090
[126] Duquesnoy M, Lombardo T, Chouchane M, Primo E N and Franco A A 2020 Data-driven assessment of electrode calendering process by combining experimental results, in silico mesostructures generation and machine learning *J. Power Sources* **480** 229103
[127] Ouyang R, Curtarolo S, Ahmetcik E, Scheffler M and Ghiringhelli L M 2018 SISSO: a compressed-sensing method for identifying the best low-dimensional descriptor in an immensity of offered candidates *Phys. Rev. Mater.* **2** 083802
[128] Primo E N, Touzin M and Franco A A 2021 Calendering of $Li(Ni_{0.33}Mn_{0.33}Co_{0.33})O_2$-based cathodes: analyzing the link between process parameters and electrode properties by advanced statistics *Batteries Supercaps* **4** 834–44

[129] Unke O T, Chmiela S, Sauceda H E, Gastegger M, Poltavsky I, Schütt K T, Tkatchenko A and Müller K R 2021 Machine learning force fields *Chem. Rev.* **121** 10142–86
[130] Shodiev A, Duquesnoy M, Arcelus O, Chouchane M, Li J and Franco A A 2021 Machine learning 3D-resolved prediction of electrolyte infiltration in battery porous electrodes *J. Power Sources* **511** 230384
[131] Fang R, Zhao S, Sun Z, Wang D W, Cheng H M and Li F 2017 More reliable lithium-sulfur batteries: status, solutions and prospects *Adv. Mater.* **29** 1–25
[132] Kilic A, Odabaşı Ç, Yildirim R and Eroglu D 2020 Assessment of critical materials and cell design factors for high performance lithium-sulfur batteries using machine learning *Chem. Eng. J.* **390** 124117
[133] Kononova O, He T, Huo H, Trewartha A, Olivetti E A and Ceder G 2021 Opportunities and challenges of text mining in materials research *iScience* **24** 102155
[134] Kononova O, Huo H, He T, Rong Z, Botari T, Sun W, Tshitoyan V and Ceder G 2019 Text-mined dataset of inorganic materials synthesis recipes *Sci. Data* **6** 203
[135] El-Bousiydy H, Lombardo T, Primo E N, Duquesnoy M, Morcrette M, Johansson P, Simon P, Grimaud A and Franco A A 2021 What can text mining tell us about lithium-ion battery researchers' habits? *Batteries Supercaps* **4** 758–66
[136] Baker M 2016 1,500 scientists lift the lid on reproducibility *Nature* **533** 452–4
[137] Li J *et al* 2020 Good practice guide for papers on batteries for the journal of power sources *J. Power Sources* **452** 227824
[138] Sun Y K 2021 An experimental checklist for reporting battery performances *ACS Energy Lett.* **6** 2187–9
[139] Stephan A K 2021 Standardized battery reporting guidelines *Joule* **5** 1–2